

COOL STARS 13: SPECTRAL CLASSIFICATION BEYOND M

S. K. Leggett¹, F. Allard², A. J. Burgasser³, H. R. A. Jones⁴, M. S. Marley⁵, and T. Tsuji⁶¹Joint Astronomy Centre Hawaii²Centre de Recherche Astronomique de Lyon³UCLA Department Physics and Astronomy⁴University of Hertfordshire⁵NASA Ames Research Center⁶Institute of Astronomy University of Tokyo

ABSTRACT

Significant populations of field L and T dwarfs are now known, and we anticipate the discovery of even cooler dwarfs by Spitzer and ground-based infrared surveys. However, as the number of known L and T dwarfs increases so does the range in their observational properties, and difficulties have arisen in interpreting the observations. Although modellers have made significant advances, the complexity of the very low temperature, high pressure, photospheres means that problems remain such as the treatment of grain condensation as well as incomplete and non-equilibrium molecular chemistry. Also, there are several parameters which control the observed spectral energy distribution — effective temperature, grain sedimentation efficiency, metallicity and gravity — and their effects are not well understood. In this paper, based on a splinter session, we discuss classification schemes for L and T dwarfs, their dependency on wavelength, and the effects of the parameters T_{eff} , f_{sed} , $[m/H]$ and $\log g$ on optical and infrared spectra. We will also discuss the various hypotheses that have been presented for the transition from the dusty L types to the clear atmosphere T types. We conclude with a brief discussion of the spectral class beyond T. Authors of each Section are identified by their initials.

Key words: Stars: atmospheres – Stars: fundamental parameters – Stars: late-type – Stars: low-mass, brown dwarfs

scheme, which has therefore become the commonly used L dwarf classification scheme.

Geballe et al. (2002) published an infrared classification scheme for L dwarfs that used a modified color–d index for types L0 to L6, the strength of the $1.5 \mu\text{m}$ wing of the H_2O absorption band for L0 to L9, and the shape of the $2.2 \mu\text{m}$ flux peak (as measured by a CH_4 index) for types L3 to L9. This scheme was pinned to the Kirkpatrick et al. and Martín et al. schemes for earlier L types and agrees reasonably well with the Kirkpatrick optical scheme, but differences of up to two subclasses do exist.

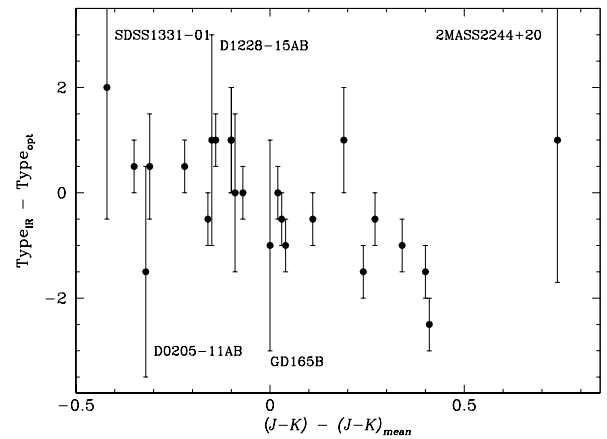


Figure 1. Difference between infrared and optical L type for a sample of L2.5 to L8 dwarfs.

1. CURRENT SPECTRAL CLASSIFICATION SCHEMES (*SKL*)

Both optical and infrared classification schemes exist for L dwarfs. In 1999, Kirkpatrick et al. and Martín et al. published optical schemes that use the strength of various features (VO 7912 Å, Rb 7948 Å, TiO 8432 Å, Cs 8521 Å, CrH 8611 Å) and pseudo-continuum slopes (the color–d 9775/7450 or PC3 8250/7560 flux ratios) to classify L dwarfs. The Martín et al. scheme terminates at L6 and the Kirkpatrick et al. at L8; types derived from the two schemes agree well except for later types, where the Martín scheme produces earlier types than Kirkpatrick. A large number of L dwarfs have been identified by the 2 Micron All Sky Survey (2MASS) and classified on the Kirkpatrick

We can understand these optical to infrared differences in terms of the effect of the silicate cloud decks that exist in the photospheres of mid- to late-type L dwarfs. For these objects, the regions of the photosphere probed by the different indices are a strong function of wavelength (see for example Figure 7 of Ackerman & Marley 2001). Where the atmosphere is opaque, e.g. in the far-red and K bands, the flux emerges from regions above the cloud decks which are less sensitive to the cloud optical depth. However the clear Z and J regions are very sensitive to the clouds. Hence the $1-2 \mu\text{m}$ infrared indices may be more indicative of cloud optical depth than T_{eff} . Also, we would expect the difference between optical and infrared type to be a function of color, as the redder, dustier, dwarfs

will suffer more veiling and hence the infrared type will be earlier than the optical type. Such a trend is seen in Figure 1 (excluding the extremely red L dwarf 2MASS2244+20 for which the optical type also seems to be affected by the clouds). The more unusually blue or red L dwarfs also show a scatter between the infrared indices, as indicated by the error bars in Figure 1 (see discussion in Knapp et al. 2004). The optical Kirkpatrick scheme terminates at L8 whereas the infrared Geballe scheme requires an L9 type. Of six infrared L9–T0 types with both optical and infrared classifications, four are optical L8s and two are L5s; one of the latter is very blue in the infrared and would be expected to have a very early L optical type.

Optical and infrared classification schemes also exist for the T dwarfs, however the optical scheme is recognised to be less accurate than the infrared schemes, and the latter are commonly used. There is little flux in the optical for the T dwarfs, making classification at these wavelengths difficult, and very few early T dwarfs have good signal to noise optical spectra, making standardisation less accurate. The optical scheme is published by Burgasser et al. (2003) and uses the Cs I 8521 Å, CrH 8611 Å, H₂O 9250 Å and FeH 9896 Å features (the last for types T5 and later only), as well as the color–e 9190/8450 flux ratio (for T2 and earlier). Infrared schemes have been published by Burgasser et al. (2002) and Geballe et al. (2002). Both use the strengths of the 1.2 μm and 1.5 μm H₂O bands, and the 1.6 μm and 2.2 μm CH₄ bands; Burgasser also uses an additional 1.3 μm CH₄ band and H/J , K/J , 2.11/2.07 flux ratios. The infrared schemes agree very well, typically to within half a subclass. The schemes are very similar and a combined scheme is in preparation (Burgasser et al.).

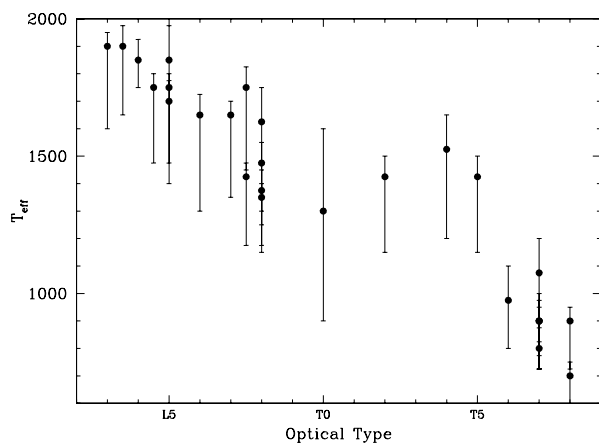


Figure 2. Effective temperatures from Golimoski et al. (2004) plotted as a function of optical L and T type.

An important issue is whether current classification schemes can be used as indicators of atmospheric parameters, such as T_{eff} . Golimoski et al. (2004) have derived

T_{eff} by integrating flux calibrated spectra for dwarfs with measured trigonometric parallaxes. Figure 6 of Golimoski et al. plots T_{eff} as a function of infrared L and T type. Figure 2 reproduces this using optical type for both the Ls and Ts. Whichever scheme is used, we find that T_{eff} is approximately constant at 1450 K for L7 to T4 types. That is, the observed spectral changes are not due to decreasing temperature, but must be explained by some other means, such as clearing of the cloud decks (see discussion in §3). Note that this implies that if the optical type is a pure indicator of T_{eff} then dwarfs with infrared type L7 to T4 should all have optical type L8. The other important atmospheric parameters, metallicity and gravity, are discussed in the next Section.

1.1. DISCUSSION (*All*)

Q: Could the derived constant T_{eff} be an error caused somehow by the breakup of the dust clouds?

A: The derivation is fairly secure as it relies on summing observed flux and well understood structural models of brown dwarf radii. [Elsewhere in these proceedings Cushing shows that the Spitzer mid-infrared results confirm the Golimoski et al. bolometric luminosities.]

Q: Can you expand on the the term “veiling”?

A: This may be misleading. The spectra of a dusty L dwarf is reddened and has weakened molecular absorption bands similar to a veiling effect. What is actually happening is that the atmosphere is heated by the dust and so the bands are formed in hotter regions and are therefore weaker. See further discussion by Allard in this session.

2. OTHER DIMENSIONS TO CLASSIFICATION

2.1. OBSERVED INDICATORS OF $[m/H]$, $\text{LOG } g$ (*AB*)

Overlapping and blanketing absorption bands from the various chemically active atomic and molecular species present in the atmospheres of cool L and T dwarfs imply emergent spectra that are particularly sensitive to metallicity and gravity effects. Gravity diagnostics have been investigated for low-mass brown dwarf candidates in young star-forming regions, which can have surface gravities 10–100 times lower than those of field dwarfs. Building from a substantial body of work on young M-type brown dwarf candidates and giant stars (e.g. Steele & Jameson 1995; Martín, Rebolo & Zapatero Osorio 1996; Luhman & Rieke 1998; Gorlova et al. 2003; Slesnick, Hillenbrand & Carpenter 2004), investigators are now searching for gravity diagnostics in young L dwarf spectra. Lucas et al. (2001) classify a number of faint Trapezium brown dwarf candidates as L-type dwarfs based on the strength of H₂O bands, calibrated against field dwarf spectra. However, the spectral morphologies of these objects are quite different from those of equivalent field dwarfs, with triangular H -band peaks and weakened Na I and CO absorption features. Near-infrared spectra of low-mass brown

dwarf candidates in σ Orionis obtained by Martín et al. (2001) are similarly classified as L dwarfs but do not show the unusual H -band morphologies. A comparison to optical spectral types obtained by Barrado y Navascués et al. (2001) for two of the σ Orionis sources suggests that near-infrared types for these low-gravity L dwarfs may be overestimated. McGovern et al. (2004) examined optical and near-infrared spectra for more reliable young cluster brown dwarf candidates and the ~ 20 – 300 Myr companion L dwarf G 196-3B (Rebolo et al. 1998; Figure 3), finding that many of the spectral features indicative of low-gravity M dwarfs and giants — enhanced metal oxides and H_2O , weak alkali lines, and weak metal hydrides — are also gravity diagnostics in the L dwarf regime. McGovern et al. used these gravity diagnostics to rule out cluster membership for at least one of the σ Orionis candidates in the Martín et al. (2001) study. Future applications of this technique may ultimately enable more reliable measures of the substellar mass function in star forming regions. A more rigorous study of L dwarf gravity diagnostics is being conducted by J. D. Kirkpatrick (priv. comm.).

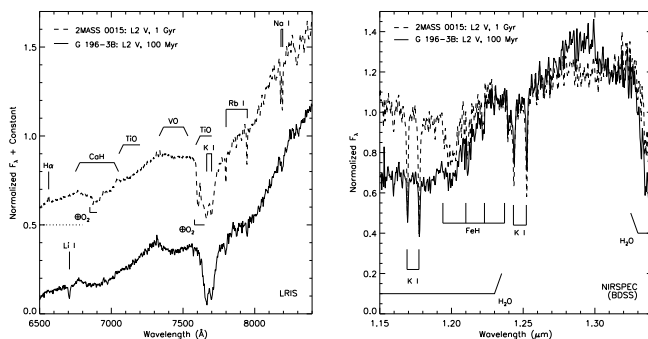


Figure 3. Low-gravity features in the 20–300 Myr L2 brown dwarf G 196-3B compared to a field L2 dwarf 2MASS 0015+35. At optical wavelengths, G 196-3B exhibits weakened alkali lines (e.g. Rb I, Na I) while TiO bands are somewhat enhanced. At near-infrared wavelengths, H_2O bands are enhanced, while alkali lines and metal hydride bands (e.g. FeH) are weaker. (Data courtesy J. D. Kirkpatrick and I. S. McLean.)

The identification of gravity features in young cluster T dwarfs has been largely impeded by their intrinsic faintness, but some progress has been made amongst higher-gravity, old and massive field brown dwarfs. Two strongly gravity-sensitive features are present in the spectra of these objects: the pressure-broadened K I and Na I fundamental doublet lines that dominate optical opacity (Burrows, Marley, & Sharp 2000) and collision-induced H_2 absorption centered around $2 \mu m$ (Saumon et al. 1994). Both features are enhanced in the spectra of higher gravity sources, while other strong molecular bands (e.g. CH_4 , H_2O) are more sensitive to T_{eff} . Variations of these fea-

tures amongst similarly classified field T dwarfs has been shown by Burgasser et al. (2005 in prep., Figure 4); while Knapp et al. (2004) have used $H - K$ color as a diagnostic for surface gravity. The near-infrared alkali lines behave in an opposite manner in T dwarfs as compared to M and L dwarfs, with weaker lines present in the spectra of higher gravity sources (Burgasser et al. 2002; Knapp et al. 2004). Only one low-gravity young cluster T dwarf candidate has thus far been identified, S Ori 70 (Zapatero Osorio et al. 2002; Martín & Zapatero Osorio 2003), although the cluster membership of this source remains controversial (Burgasser et al. 2004). A low-gravity field T dwarf may have recently been identified in the SDSS survey by Knapp et al. (2004).

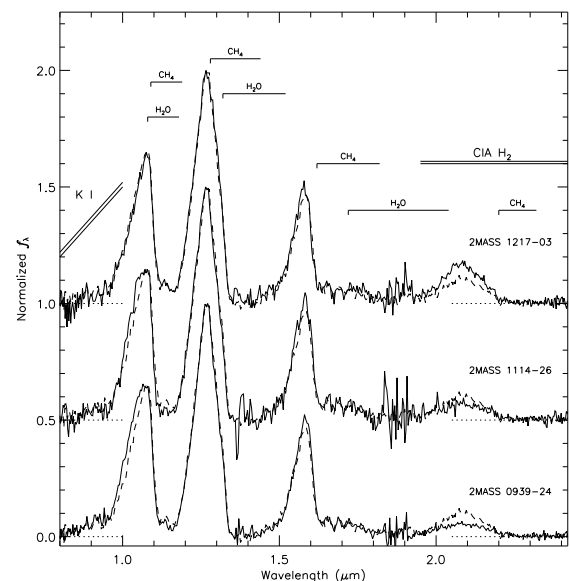


Figure 4. Low resolution near-infrared spectra of T dwarfs showing variations in gravity-sensitive features. All of the objects plotted as solid lines are classified T7.5 based on the strength of H_2O and CH_4 band strengths and have similar spectral morphologies to the 2–5 Gyr T7.5 companion brown dwarf Gliese 570D (Burgasser et al. 2000; dashed lines). Two exceptions are the $1 \mu m$ peak, shaped by the pressure-broadened wings of K I, and the $2.2 \mu m$ peak, controlled by collision-induced H_2 absorption. (Adapted from Burgasser et al. in prep.)

Metallicity spectral signatures have only recently been explored among newly identified L-type halo subdwarfs. One of the first discoveries, 2MASS 0532+8246 (Burgasser et al. 2003), has an optical and J -band spectral morphology reminiscent of a late-type L dwarf, but exhibits a highly suppressed K -band peak due to enhanced H_2 absorption. As a result, this object has near-infrared colors more typical of late-type T dwarfs ($J - K \sim 0.3$). 2MASS 0532+8246 also exhibits enhanced hydride bands

and broadened alkali lines, typical characteristics of late M-type subdwarfs. Two other L subdwarfs have since been identified (Lepine, Rich, & Shara 2003; Burgasser 2004). Further discussion on L and T subdwarfs can be found in the contribution by A. J. Burgasser (these proceedings). No unambiguous halo (and hence metal-poor) T dwarf has yet been identified, although the unusually blue ($J - K = -1.1$; Golimowski et al. 2004) 2MASS 0937+2931 (Burgasser et al. 2002) is a good candidate.

2.2. THEORETICAL INDICATORS OF $[m/H]$, $\text{LOG } g$ (FA)

Brown dwarfs, unlike main sequence stars, do not define a unique spectral sequence. Instead luminosity is a function of age, mass and composition. This implies a dependency between effective temperature, surface gravity and composition. It is important to be able to disentangle spectral changes caused by changes in these three parameters. In this section, we explore the response of our synthetic spectra to gravity and metallicity changes in the two charac-

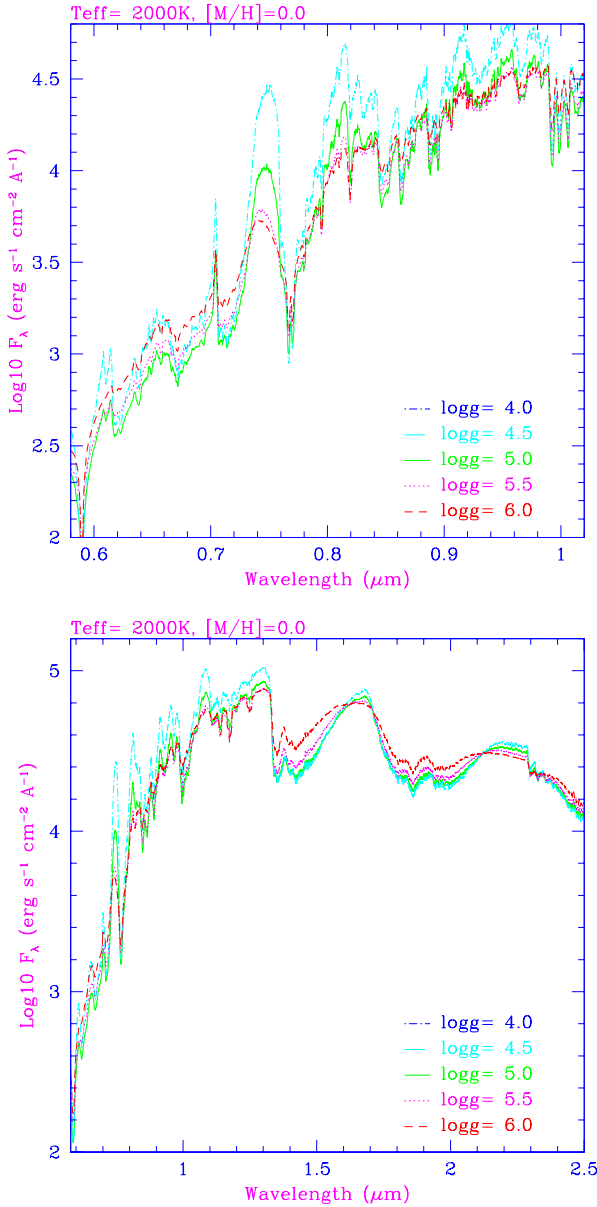


Figure 5. AMES-Dusty-2001 models for $T_{\text{eff}} = 2000 \text{ K}$, $[m/H] = 0.0$ for $\text{logg} = 4.0$ to 6.0 in the optical (top) and infrared (bottom). With increasing gravity, the dust scattering continuum increases, producing a backwarming that decreases the TiO and H_2O band strengths (cf. Fig.3).

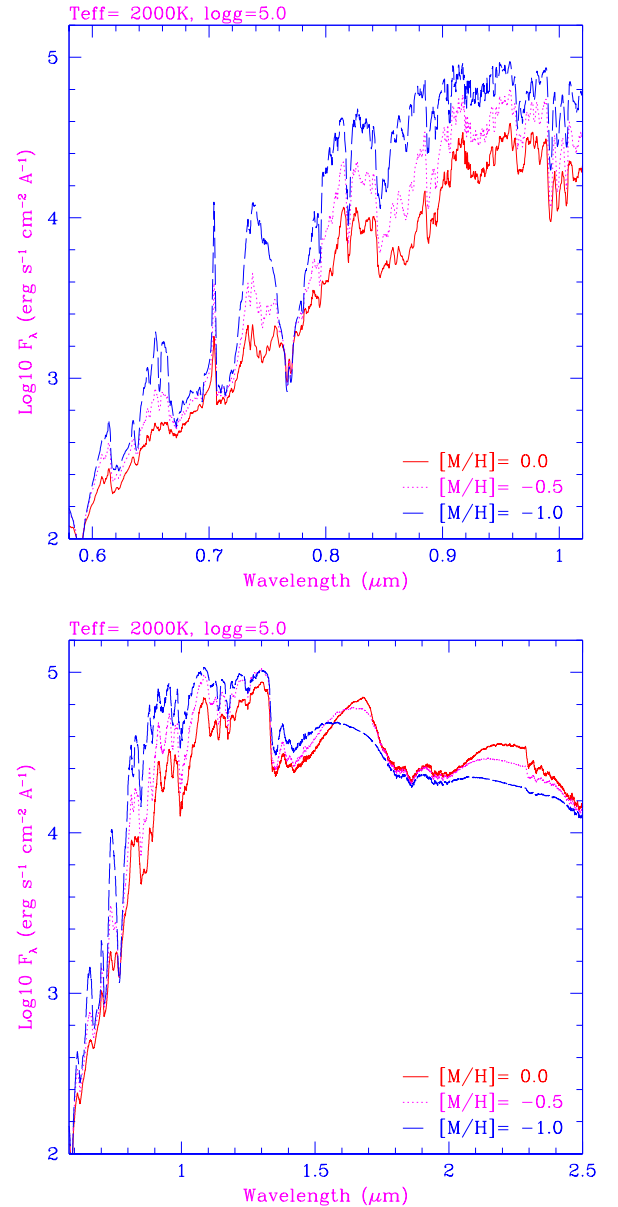


Figure 6. AMES-Dusty v2.7 models for $T_{\text{eff}} = 2000 \text{ K}$, $\text{logg} = 5.0$ for $[m/H] = 0.0, -0.5, -1.0$ in the optical (top) and infrared (bottom). With decreasing metallicity, the dust scattering, TiO and VO opacities decrease, and H_2 opacity increasingly depresses the H and K flux peaks.

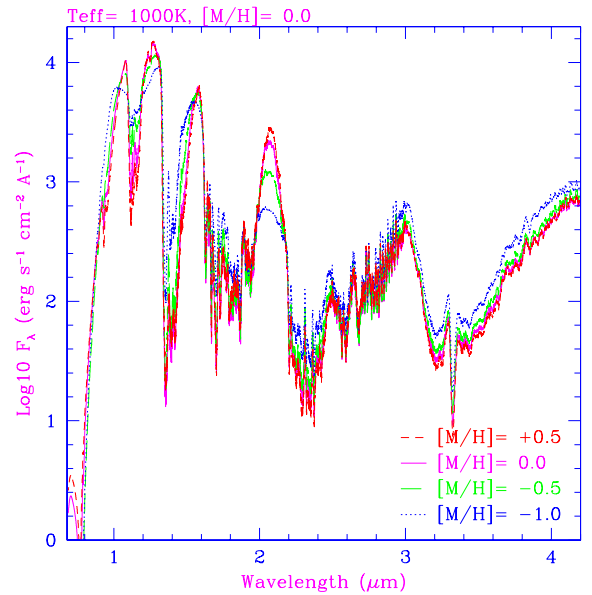
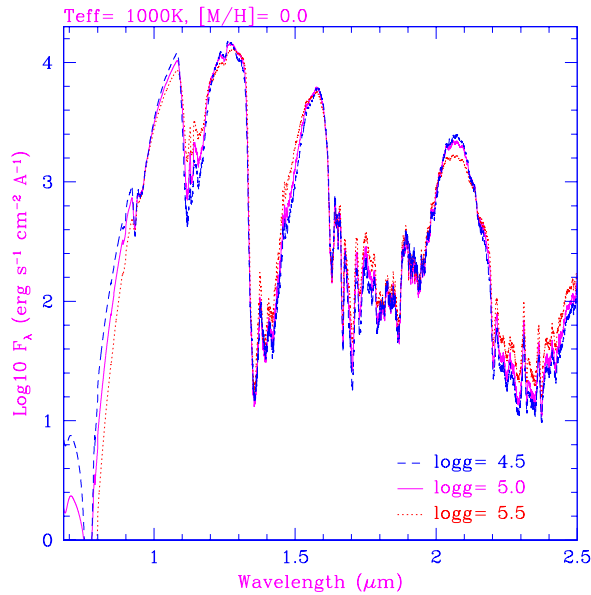
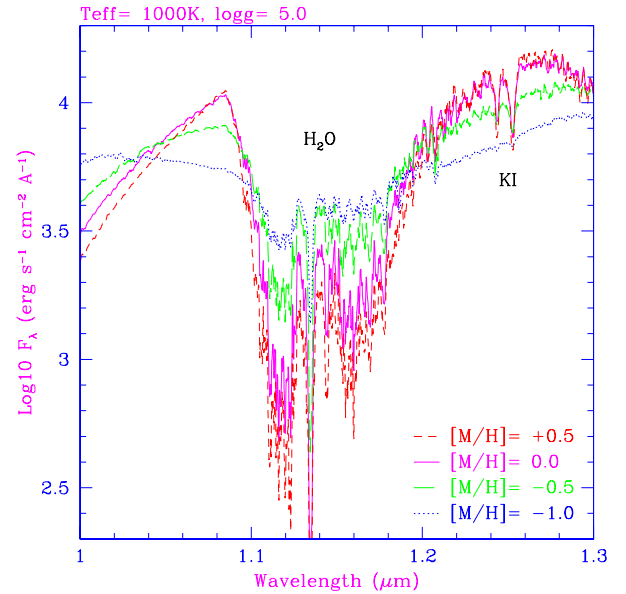
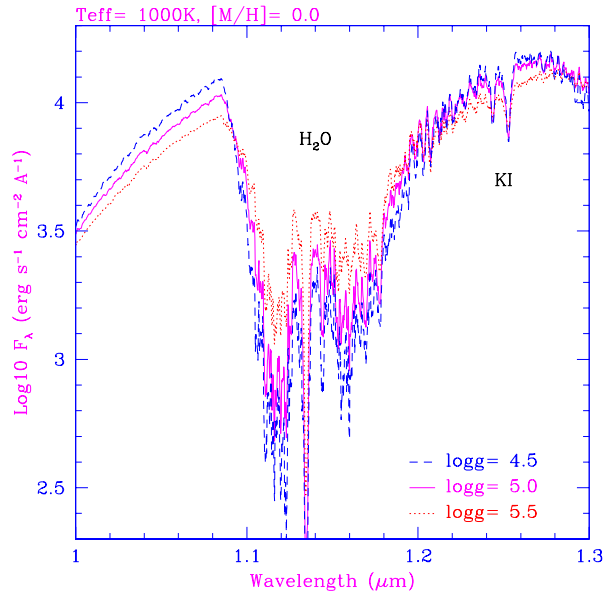


Figure 7. AMES-Rainout models using detailed Na ID and $0.77 \mu\text{m}$ K I line profiles (Allard et al. 2003) for $T_{\text{eff}} = 1000 \text{ K}$, $[M/H] = 0.0$ are compared for $\log g = 4.5$, 5.0 and 5.5 . With increasing gravity, the broadening of the K I doublets at 0.77 and $1.25 \mu\text{m}$ increases with gas pressure. The K-band flux peak is depressed by increasing H_2 opacity, and the strengths of the 1.14 and $2.3 \mu\text{m}$ H_2O bands decrease (cf. Figure 4).

teristic regimes of dusty and dust free atmospheres, i.e. in the M to L type dwarf regime, and in the T dwarf regime. We avoid the intermediate regime at T_{eff} between 1700 and 1400 K , where partial cloud coverage and/or formation may prevail, which is discussed in §3.

Here we show plots demonstrating the effects of gravity ($\log g$) and metallicity ($[M/H]$). We use new extensions of

Figure 8. AMES-Rainout models for $T_{\text{eff}} = 1000 \text{ K}$, $\log g = 5.0$ and $[M/H] = +0.5, 0.0, -0.5$ and -1.0 . With decreasing metallicity, the broadening of the Na ID and $0.77 \mu\text{m}$ K I first increases with pressure. This produces backwarming at longer wavelengths causing hotter H_2O and CH_4 bands characterized by weaker, broader bands (especially at 1.14 and $1.4 \mu\text{m}$). The contrast of the K I doublet at $1.25 \mu\text{m}$ thus appears to decrease with decreasing metallicity. The K-band peak is depressed by increasing H_2 opacity. The blue wing of the Z-band peak at $1.09 \mu\text{m}$ is determined by the K I $0.77 \mu\text{m}$ red wing, which for $\lambda > 0.88 \mu\text{m}$ shows an unexpected decrease with decreasing metallicity most likely due to backwarming effects.

the Dusty models grid to a wide range of metallicity, and also a new grid of dust-free models where the grain opac-

ities have not only been neglected (Cond-style models), but where the chemical equilibrium has been systematically depleted of all grains (Rainout models). These models also include new detailed line profiles for the Na I D and K I doublets at 0.59 and 0.77 μm (Allard et al. 2003).

The models indicate that an increase in gravity produces similar spectral changes to a decrease in metallicity, since both these changes increase the gas pressure in the atmosphere. However, the presence of dust grains in the atmospheres of late M to L dwarfs, which responds strongly to a decrease in metallicity, reverses the behavior of optical to red spectral features allowing the effects to be separated. This is not the case for the dust-free T dwarfs which behave much more like M subdwarfs.

The changes in the strength and width of the most prominent spectral features as a function of surface gravity and metallicity for these two cases are reported in Table 1. Changes in the shape and brightness of the inter-band flux peaks at 1.3, 1.6 and 2.2 μm (labeled *J*, *H* and *K* respectively), and caused by the local temperature-dependance of the shape of the water bands, are also reported. Note that the width of the optical K I and Na I D lines and the pressure-induced absorption by H_2 in the *K* bandpass both increase with increasing mass density of the plasma.

Table 1. Summary of Effects of Gravity and Metallicity

T_{eff}	$\rho \uparrow$	Lines	Grains	TiO	H_2O	H_2	<i>J</i>	<i>H</i>	<i>K</i>
K				VO	CH_4				
2000	$g \uparrow$	\uparrow	\uparrow	\downarrow	\downarrow	\uparrow	\downarrow	\downarrow	\downarrow
2000	$z \downarrow$	\uparrow	\downarrow	\downarrow	$=$	\uparrow	\uparrow	\downarrow	\downarrow
1000	$g \uparrow$	\uparrow	\downarrow	\uparrow	$=$	$=$	\downarrow
1000	$z \downarrow$	\uparrow	\downarrow	\uparrow	\downarrow	$=$	\downarrow

2.3. DISCUSSION (*All*)

Q: It does seem that distinguishing between the various parameters requires a good set of e.g. age calibrators.
A: Unfortunately most of the new L and T dwarfs are free-floating isolated objects. But some things help — even if metallicity and gravity produce the same effect, the size of the effect can be very different. Note also that if metallicity is reduced it affects the double-metal features (e.g. TiO, VO) more than the single-metal features (e.g. K I, H_2O).
Q: We should ensure that any label for gravity, e.g. *abc*, provides sufficient range to cover all expected gravities.
A: This is true. Eventually we should use a roman numeral giving an actual value in cgs units, as for the stars.
Q: Do the speakers have favorite metallicity or gravity indicators?

A: The shape of the *ZJHK* flux peaks are very useful, as are the K I lines and the H_2O wings. We also need to obtain a large enough sample to find the outliers with

extreme metallicity and/or gravity. One way to do this is through proper motion surveys which can identify the older, likely metal-poor dwarfs.

3. THE TRANSITION FROM L TO T

3.1. THE SINKING HOMOGENEOUS CLOUD (*TT*)

In the photosphere of ultracool dwarfs, we assume that dust forms at the condensation temperature T_{cond} but soon segregates at slightly lower temperature which we referred to as the critical temperature T_{cr} . As a result, a dust cloud forms in the region where $T_{\text{cr}} \lesssim T \lesssim T_{\text{cond}}$, and this model is also referred to as the Unified Cloudy Model (UCM, Tsuji 2002). Since $T_{\text{cond}} \approx 2000\text{K}$ for iron grains, for example, the dust cloud forms in the optically thin region of L dwarfs whose T_{eff} 's are relatively high, but in the optically thick region of T dwarfs whose T_{eff} 's are relatively low. As a result, it looks as if a homogeneous cloud formed in the upper photospheric layer in L dwarfs sinks to the deeper layer in T dwarfs. As long as the homogeneous cloud is in the upper photosphere as in L dwarfs, it will directly effect the observables and explains why L dwarfs appear to be dusty. In T dwarfs, the effect of dust on the observables diminishes as the dust cloud sinks to the deeper region and, to a first approximation, this immersion of the homogeneous cloud explains the transition from L to T. Note, however, that no specific mechanism is assumed for the sinking of the homogeneous cloud, this is simply a natural consequence of the change of the thermal structure as L dwarfs evolve to T dwarfs.

This is clearly shown in Figure 9 where *J* – *K* (Knapp et al. 2004) is plotted against T_{eff} based on the bolomet-

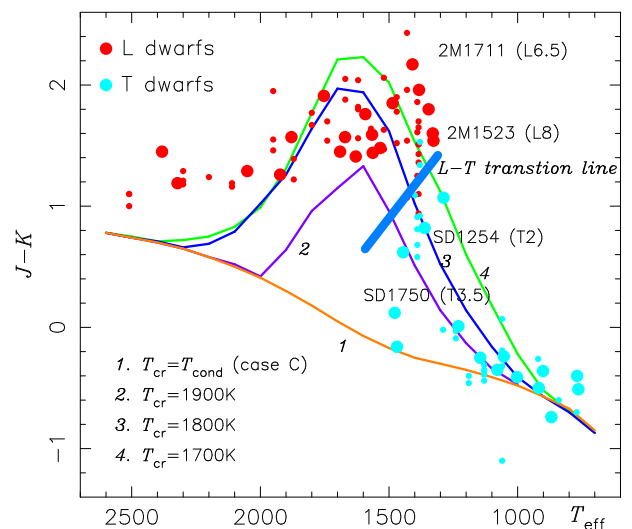


Figure 9. *J* – *K* (Knapp et al. 2004) plotted against T_{eff} (Vrba et al. 2004), and the predicted colors based on the UCMs with $\log g = 5.0$ and $T_{\text{cr}} = T_{\text{cond}}$ (case C), 1900, 1800, and 1700 K. The L – T transition line is indicated.

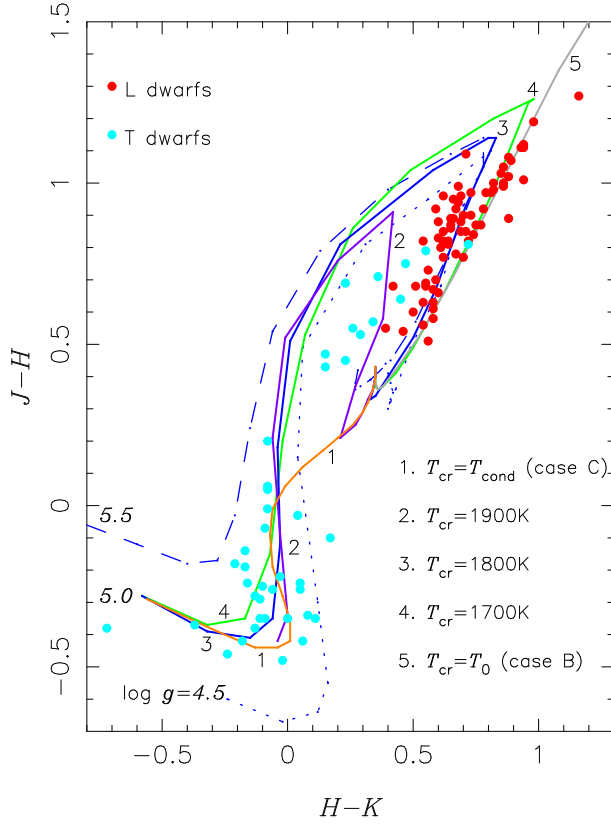


Figure 10. Observed $(J - H, H - K)$ (Knapp et al. 2004) compared with the predicted colors based on the UCMs with $T_{\text{cr}} = T_{\text{cond}}$ (case C), 1900, 1800, 1700 K, and T_0 (case B) under the fixed value of $\log g = 5.0$, and those for $\log g = 4.5$ (dotted line) and 5.5 (dashed line) with the fixed value of $T_{\text{cr}} = 1800$ K. Note that $700 \leq T_{\text{eff}} \leq 2600$ K throughout.

ric flux (Leggett et al. 2002, Golimowski et al. 2004, Vrba et al. 2004), with different symbols for L and T dwarfs. The predicted values of $J - K$ for several values of T_{cr} are overlaid. The lower value of T_{cr} implies that the homogeneous cloud is thicker and $J - K$ will be redder because of the increased dust extinction. The scatter of the observed $J - K$ at any T_{eff} is rather large and this means that T_{cr} is variable at a fixed T_{eff} . After all, both T_{eff} and T_{cr} change in the transition from L to T across the “L—T transition line” indicated by the thick line in Figure 9.

In Figure 10, the observed $(J - H, H - K)$ (MKO system, Knapp et al. 2004) is compared with the predicted values for several values of T_{cr} at the fixed value of $\log g = 5.0$. The cases of $\log g = 4.5$ and 5.5 are shown by the dotted and dashed lines, respectively, at the fixed value of $T_{\text{cr}} = 1800$ K. Inspection of Figure 10 reveals that the spread of the observed data in L and early T dwarfs is explained by the continuous change of T_{cr} from T_{cond} to T_0 (surface temperature) while that in late T dwarfs by the effect of $\log g$. Thus, observed two-color diagrams can be explained with the three parameters, T_{eff} , $\log g$, and T_{cr} , but cannot with the two parameters, T_{eff} and $\log g$ alone.

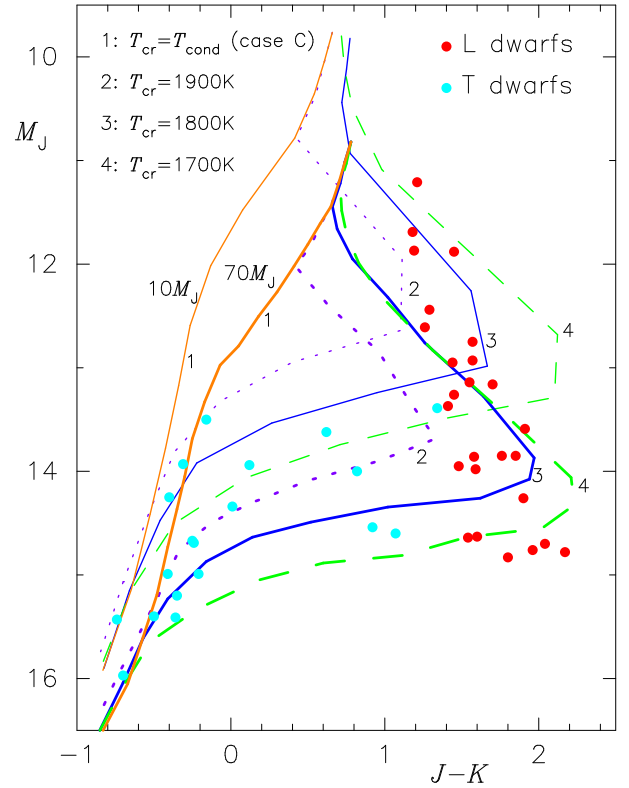


Figure 11. Observed $(J - K, M_J)$ diagram (Knapp et al. 2004) compared with predicted loci which are transformed from evolutionary tracks (Burrows et al. 1997) of $M/M_{\text{Jupiter}} = 10$ (thin lines) and 70 (thick lines), via the UCMs with $T_{\text{cr}} = T_{\text{cond}}$ (case C), 1900, 1800 and 1700 K.

Characteristic features of the observed $(J - K, M_J)$ color-magnitude (CM) diagram (Dahn et al. 2002, Tinney, Burgasser & Kirkpatrick 2003, Vrba et al. 2004) shown in Figure 11 are rapid bluing and brightening at the transition from L to T. We transform the theoretical $(T_{\text{eff}}, M_{\text{bol}})$ diagrams for initial masses of 10 and 70 M_{Jupiter} (Burrows et al. 1997) to the $(J - K, M_J)$ diagram via UCMs with $T_{\text{cr}} = T_{\text{cond}}$, 1900, 1800, and 1700 K, instead of the previous attempt assuming a uniform value of $T_{\text{cr}} = 1800$ K throughout (Tsuji & Nakajima 2003), and the results are overlaid on Figure 11. It is found that almost all the observed data can be reproduced with our predictions, and the bluing and brightening of the early T dwarfs can be explained by the models of $T_{\text{cr}} \approx T_{\text{cond}}$ (i.e. effectively no cloud) if not by the very low-mass models. Thus the L—T transition on the CM diagram can be explained with the sinking homogeneous cloud model, but only if a sporadic variation of T_{cr} , which is a measure of the thickness of the cloud (or dust column density) in the observable photosphere, is assumed. Such a variation of T_{cr} is not predicted by the present theory of structure and evolution of substellar objects, but we had to introduce T_{cr} as

a free parameter to interpret purely empirical data such as the two-color diagram and CM diagram.

The change of the spectra at the transition from L to T could have been interpreted as due to the change of T_{eff} on the assumption of $T_{\text{cr}} = 1800\text{K}$ throughout

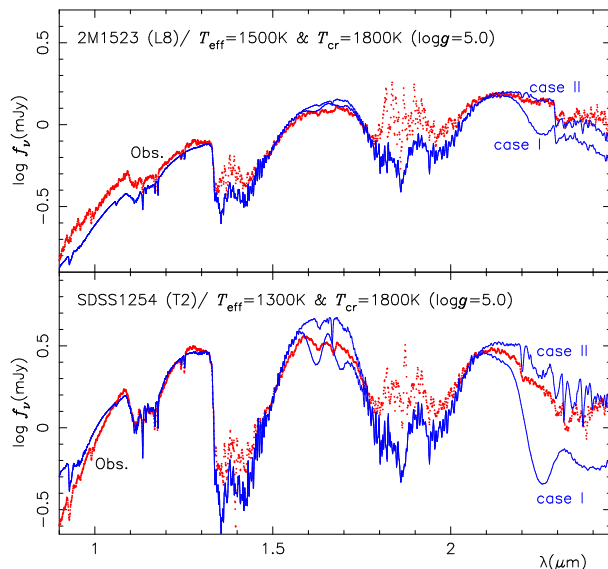


Figure 12. The spectral change at the transition from L to T, exemplified by 2MASS 1523 (L8) and SDSS 1254 (T2), can be interpreted as due to the change of T_{eff} under the fixed value of $T_{\text{cr}} = 1800\text{K}$. Observed and predicted spectra are shown by dots and solid lines, respectively.

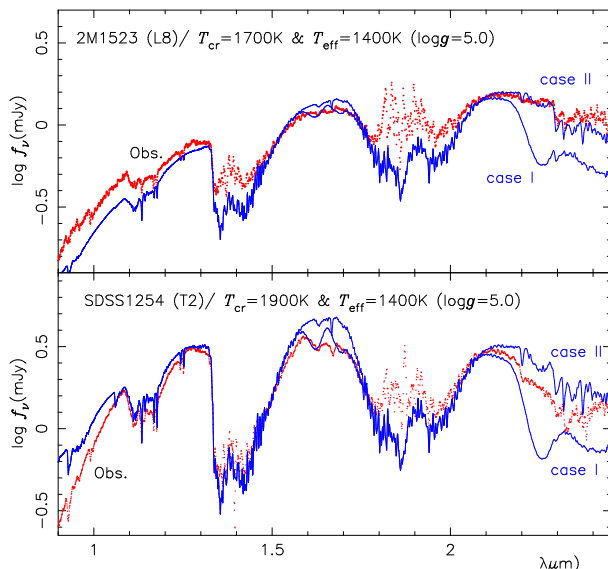


Figure 13. The spectral change at the transition from L to T, exemplified by 2MASS 1523 (L8) and SDSS 1254 (T2), can also be interpreted as due to the change of T_{cr} under the fixed value of $T_{\text{eff}} = 1400\text{K}$. Observed and predicted spectra are shown by dots and solid lines, respectively.

(Tsuji, Nakajima & Yanagisawa 2004). For example, the typical L dwarf 2MASS 1523 showing red colors and weak or no CH_4 bands could be consistent with $T_{\text{eff}} = 1500\text{K}$, while the early T dwarf SDSS 1254 showing strong H_2O and modest CH_4 bands with $T_{\text{eff}} = 1300\text{K}$ (Figure 12). However, infrared colors suggest that T_{cr} cannot be the same throughout L—T dwarfs (Figure 9) and also empirical values of T_{eff} show a plateau at $T_{\text{eff}} \approx 1400\text{K}$ between L8 and T4 (Golimowski et al. 2004, Vrba et al. 2004). For this reason, we examine if the same spectra at the L—T transition can be explained with $T_{\text{eff}} \approx 1400\text{K}$ throughout but with changing T_{cr} . The L8 dwarf 2MASS 1523 can be explained with $T_{\text{cr}} = 1700\text{K}$ while the T2 dwarf SDSS 1254 with $T_{\text{cr}} = 1900\text{K}$ (Figure 13). Thus, different combinations of T_{eff} and T_{cr} could explain the change of spectra at the transition from L to T. This is because the dust column density in the observable photosphere depends not only on T_{eff} but also on T_{cr} .

How can we decide which case is correct? For this purpose, assume first the empirical T_{eff} based on the bolometric flux, and T_{cr} can be estimated based on the infrared colors (Figure 9). Also, transform the observed spectrum to the spectral energy distribution (SED) on an absolute scale with the use of the observed parallax. Then, analyze the SED to improve T_{eff} , T_{cr} , $\log g$, chemical composition, v_{micro} , etc. Such an analysis applied to a sequence of L—T dwarfs including 2MASS1711 (L6.5), 2MASS 1523 (L8), SDSS 1254 (T2), and SDSS 1750 (T3.5), which could have been interpreted as a sequence of T_{eff} from 1800 to 1100 K with the uniform value of $T_{\text{cr}} = 1800\text{K}$ (Tsuji, Nakajima & Yanagisawa 2004), revealed that $T_{\text{eff}} \approx 1300\text{K}$ throughout but T_{cr} should change from 1700 K to T_{cond} (Tsuji, these proceedings). It is surprising that the distinct changes of the spectra from L6.5 to T3.5, including the L—T transition, are nothing to do with T_{eff} but are instead due to the change of the dust column density at fixed T_{eff} . This result that the L—T spectral sequence is not a temperature sequence is based on a limited sample, but the same conclusion can be suggested by the curious brightening of M_J when plotted against the L—T types.

The transition from L to T takes place at $T_{\text{eff}} \approx 1400 \pm 100\text{K}$ (Figures 2, 9), and this transition can be understood as a consequence of a homogeneous cloud effectively sinking from optically thin to thick regions at about this T_{eff} . However, the L—T transition appears to be a somewhat more complicated phenomenon in that T_{cr} also changes (Figure 9) and this is even more directly related to the L—T spectral types around the transition. In other words, the thickness of the homogeneous cloud appears to decrease and even disappear at the transition from L to T. However, the mechanism of how T_{cr} changes at $T_{\text{eff}} \approx 1400\text{K}$ is unknown. The only known change of the photospheric structure is the formation of the second (surface) convective zone at $T_{\text{eff}} \approx 1400\text{K}$ in the UCMS (Tsuji 2002). The exact meaning of the transition from L to T remains unsolved until the origin of the sporadic variation of T_{cr} can

be identified. Moreover, the meaning of the L—T spectral classification as a whole should be reconsidered in view of the difficulty of interpreting it as a temperature sequence.

3.2. OTHER MODELS FOR THE TRANSITION (*MSM*)

A sufficient number of late L to early to mid T dwarfs (approximately L8 to T5) have now been found that a number of characteristics of the transition can be listed.

- *Turn to the blue in $J - K$* The colors of L dwarfs become progressively redder until they saturate at $J - K \sim 2$ at spectral type L8 (Knapp et al. 2004). This color then rapidly turns to the blue, reaching $J - K \sim -0.8$ by T8 or so.
- *Color change at near constant T_{eff}* Recent estimates of the bolometric T_{eff} from Golimowski et al. (2004, made possible by the parallax measurements of Vrba et al. 2004) have quantified the speed of this color change, as shown in Figures 9 and 14. Most ($> 80\%$) of the change in $J - K$ color is seen to occur over a very small T_{eff} range near 1300 K. This is a remarkable result as it implies that brown dwarfs are undergoing substantial spectral and color changes over a very small temperature range.
- *Brightening at J* The L to T transition also appears to be associated with a brightening at J from late L to early T (T4 or so, Knapp et al. 2004). H , K , L , and M bands show no sign of such brightening (Knapp et al. 2004, Golimowski et al. 2004), while there is some evidence of a brightening at Z . It should be noted that the bolometric luminosity, as would be expected, does *not* increase across the transition.
- *Resurgence of FeH* Burgasser et al. (2002) argue there is evidence that the $0.997 \mu\text{m}$ FeH band, after decaying away as FeH is presumably lost to Fe drops and grains, shows a resurgence in strength, coincident with the $J - K$ color change.
- *Model spectral fits* The comparison of models and data as shown by Tsuji in the previous section and by Marley et al. elsewhere in these proceedings shows that while cloudy models fit the L dwarfs, by spectral type T5 models with no cloud opacity (but with condensation included in the equilibrium chemistry) fit spectra very well, implying that condensates play a very small role in controlling the thermal profile and emitted flux of mid- to late-T dwarfs.

Any explanation of the L to T transition mechanism must be consistent with the evidence summarized above. The unmistakable gross explanation – that condensates have been lost from the atmosphere – belies the difficulty in explaining this loss in a self-consistent manner. That a sinking, finite-thickness cloud deck will eventually disappear from sight allowing the atmosphere above to cool has been apparent for some time (Allard et al 2001, Marley 2000, Tsuji & Nakjima 2003). The difficulty lies in explaining the rapidity of the color change in light of the

measured effective temperatures (Figures 9 and 14). The cloud model of Ackerman & Marley (2001) while nicely accounting for the $J - K$ colors of the reddest L dwarfs takes much too long to ultimately sink out of sight (Burgasser et al. 2003, Knapp et al. 2004).

Tsuji (2002) and Tsuji et al. (2004) proposed that a physically thin cloud, thinner than predicted by the Ackerman & Marley model, could self-consistently explain the rapid L to T transition. These UCM models indeed exhibit a faster L- to T-like transition, but as Figure 9 demonstrates these models, with fixed T_{cr} , are not consistent with the observed rapidity of the color change. Even accounting for a likely spread in gravities across the transition cannot account for the observations. In addition the UCM models, like the cloudy models of Marley et al., do not brighten in J band across the transition. Tsuji now suggests (§3.1) that T_{cr} must vary across the transition, allowing the cloud to essentially collapse as $T_{\text{cr}} \rightarrow T_{\text{cond}}$.

To overcome the sort of difficulties faced by the Tsuji et al. models, Burgasser et al. (2002), following a suggestion from Ackerman & Marley (2001), hypothesized that the transition was associated with the appearance of holes in the global cloud deck. The holes, hypothesized to be similar to Jupiter’s well known “5-micron hot spots”, would allow flux to emerge through the Z - and J -band atmospheric opacity windows. If the onset of the holes corresponded with the T_{eff} of the L/T transition region, then their appearance could account for the characteristics of the transition outlined above. Indeed Burgasser et al. demonstrated with a simple model that holes could

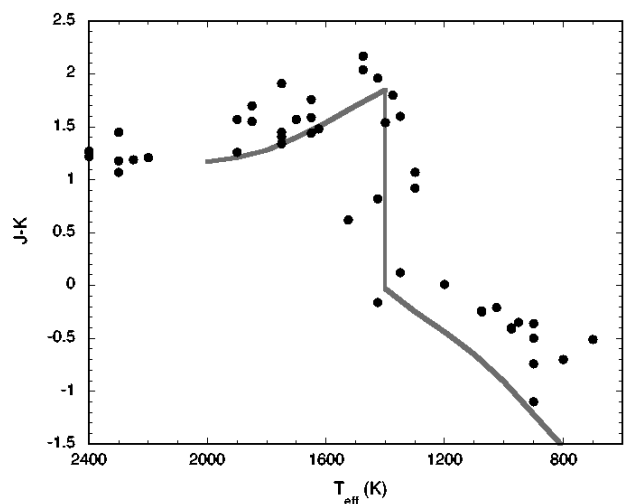


Figure 14. Ultracool dwarf MKO $J - K$ and T_{eff} (Knapp et al. 2004 and Golimowski et al. 2004). Model curve is a composite of cloudy (for $T_{\text{eff}} \geq 1400$ K) and clear (for $T_{\text{eff}} \leq 1400$ K) models (Marley et al. 2002) connected by a vertical line at $T_{\text{eff}} = 1400$ K, all for $\log g = 5$.

plausibly account for the bluing in $J - K$ and brightening in J . Figure 14, similar to Figure 9, demonstrates that, for fixed gravity, rapidly moving from a cloudy to a cloud-free model apparently accounts for the available data. This mechanism would also account for the reappearance of FeH absorption since hot, FeH-bearing gas would be detectable through the clouds, if the holes pierced both the global silicate and underlying Fe cloud deck.

Finally Knapp et al. (2004) suggested that, like a varying T_{cr} , a varying f_{sed} (sedimentation efficiency, Ackerman & Marley 2001) could result in a sudden downpour that might rapidly remove the cloud deck over a small effective temperature range.

Regardless of whether the L to T transition is explained by the appearance of holes in the global cloud deck or a sudden increase in the efficiency of condensate sedimentation, the root cause must lie with the atmospheric dynamics. Perhaps the behavior of condensates change when the cloud reaches a certain depth in the atmospheric convection zone. When even the cloud tops are firmly rooted in the convection zone the clouds may be sheared apart by height-varying zonal flow, like that found in Jupiter. Perhaps the second, detached convection zone found in brown dwarf atmosphere models plays a role. Another possibility is that there is a change in the global atmospheric circulation that affects the cloud decks. Schubert & Zhang (2000) found that brown dwarfs likely exhibit one of two styles of global atmospheric circulation. They may either exhibit circulation strongly influenced by rotation, like Jupiter, or fairly independent of rotation, like the Sun. Perhaps the L to T transition is associated with a transition between the two circulation regimes encountered as a brown dwarf cools. The solution of this enigma certainly lies in understanding the three dimensional interplay of global atmospheric circulation with both macro- and micro-scale cloud dynamics.

3.3. DISCUSSION (*All*)

Q: We need to see the L to T transition in clusters to reduce the age spread in the color:magnitude diagram.

A: Work done on the σ Ori cluster is probing into the T regime and may show the blueward turn in the diagrams.

Q: The change in spectral type at constant effective temperature is a real and observed effect; it is not artificial.

A: Its artificial only in the sense that it is due to changing cloud parameters and not changing T_{eff} .

Q: Is it OK to have spectral type *not* depend on T_{eff} ?

A: In the spirit of the spectral type being an observable, yes it is. The spectra definitely change.

Q: Is there a correlation between T_{cr} and f_{sed} ?

A: No because there are differences between the two models such as particle size. Note that no set of parameters for particle size can explain the L to T transition.

Q: Surely microphysical effects should be included?

A: This is very complex and we try to mimic the ef-

fects through the T_{cr} and f_{sed} parameters. [Discussion of the microphysics is presented by Hellings elsewhere.]

Q: Is the mixing length approximation to convection valid?

A: It is acceptable to first order for L and T dwarfs. The plane parallel assumption is OK too.

Q: For Jupiter we see that the holes are significant flux contributors.

A: The L and T dwarfs are being monitored for variability. Interpreting the results depends however on both hole size and number.

4. SPECTRAL TYPES BEYOND T (*HRAJ*)

The concepts and nomenclature of stellar classification were refined in the late 19th century primarily through the works of Secchi, Fleming and Pickering. The sequence of letters used today comes from the work of Canon & Pickering (1901) who produced the OBAFGKM empirical sequence based on differences between photographic spectra. This sequence has been embellished with further spectral types, e.g. C to denote carbon stars (Morgan, Keenan & Kellman 1941), but served as a complete temperature sequence for nearly a hundred years. Then in the 1990s intrinsically faint very cool objects started to be discovered (e.g. GJ 229B by Nakajima et al. 1995). The spectra of objects such as GJ 229B (e.g. Oppenheimer et al. 1995 and Figure 15) showed unprecedented methane-rich spectra. Such spectra along with the burgeoning numbers of M dwarfs with spectral types beyond M9 (Kirkpatrick et al. 1998) gave rise to the necessity for further spectral types.

The letter L results from a proposal by Martín et al. (1997) that L should denote Low temperature and there might be Low temperature lithium and methane designations. The L spectral type and also the T spectral type became generally accepted in the literature following a seminal paper by Kirkpatrick et al. (1999) and a meeting dedicated to the “Ultracool Dwarfs: New Spectral Types

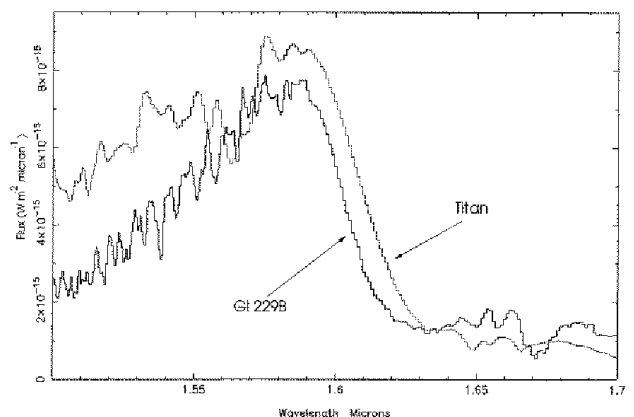


Figure 15. Spectra of GJ 229B (solid line) and Titan (scaled by a factor of 0.003) near the $1.6\mu\text{m}$ methane absorption edge (credit - Geballe et al. 1996).

L and T” (Jones & Steele 2001). Despite these relatively recent introduction of new spectral classifications, even more recent discoveries of very faint red objects, supported by infrared spectra and parallaxes (Burgasser et al. 2002, Geballe et al. 2002, Golimowski et al. 2004, Knapp et al. 2004, Tinney et al. 2003, Vrba et al. 2004) indicate that a spectral type of T8 or T9 has been reached. It is thus important to consider further spectral types.

Notwithstanding the non-alphabetical order of the hot spectral types, it seems desirable to continue the sequence alphabetically when suggesting further, cooler, types. Thus a letter from T to Z would be preferred, though perhaps not Z itself as this suggests the end of the spectral typing sequence. There are three major factors to consider in choosing a new spectral type: (1) it must be unambiguous and should not currently be used to represent any other spectral type, (2) the letter must represent a typing that is clearly distinguished from other types of astronomical objects, (3) the letter should be free of physical interpretation (which is likely to vary with time). As discussed by Kirkpatrick et al. (1999), U and X are problematic choices because of possible associations with Ultraviolet and X-ray sources. V would be a good choice but for the possible confusion with vanadium oxide (VO) which shows prominent bands in spectra of late-type M and early-type L dwarfs.

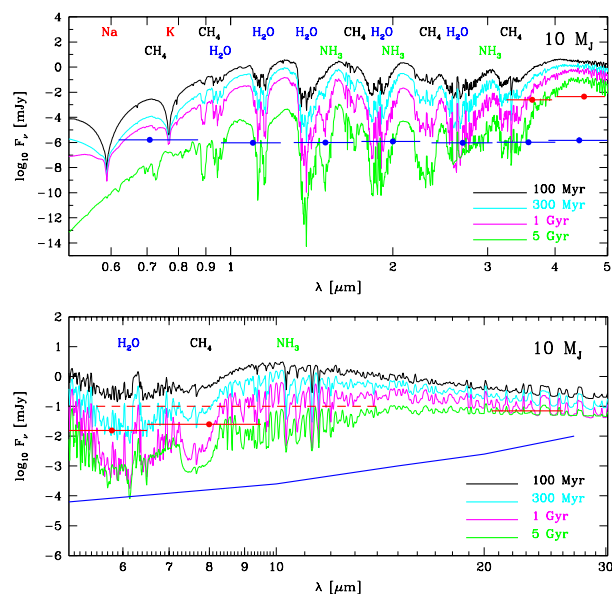


Figure 16. Spectra of $10 M_{\text{Jup}}$ brown dwarfs at 1, 3 and 5 billion years. the SIRTUF and JWST detector sensitivities are plotted for reference. Gaseous water absorption features remain strong over this range of ages. Methane and ammonia absorption features strengthen with age, as the alkali lines wane. The wavelength positions of various of the molecular and atomic features are depicted for reference. (credit - Burrows et al. 2003).

W is undesirable because of likely confusion with Wolf-Rayet WN and WR classes. Y could be confused with yttrium oxide (YO) which may also appear in cool dwarf spectra, however, it has yet to be identified and the low abundance of YO means that it may not be evident. Assuming that YO is not found, Y seems the best choice for the next spectral class. While the choice of Y may seem uncomfortably close to the end of the alphabet it is important to note that the broad spectral features of T dwarfs are somewhat similar to the solar system planets Titan and Jupiter. Although the infrared spectra of solar system objects are in reflected sunlight, their spectra are dominated by methane and water vapour absorption features in a similar manner to T dwarfs, e.g. Figure 15. In fact, given the relatively low masses and temperatures of Titan and Jupiter it is perhaps desirable that the classification system is reaching an alphabetic end point.

The dominance of methane in the infrared spectra of T dwarfs means they are often called methane dwarfs. While methane is the defining characteristic of T dwarfs it can also be seen at $3.3 \mu\text{m}$ in L spectral types later than L4 (Noll et al. 2000). Recently obtained mid-infrared spectra (Roellig et al. 2004) show that ammonia can be seen at $11 \mu\text{m}$ in T dwarfs later than T5. Figure 16 from Burrows, Sudarsky & Lunine (2003) indicates that ammonia will become dominant in both the near- and mid-infrared at temperatures below 700 K. It is likely that, in the same

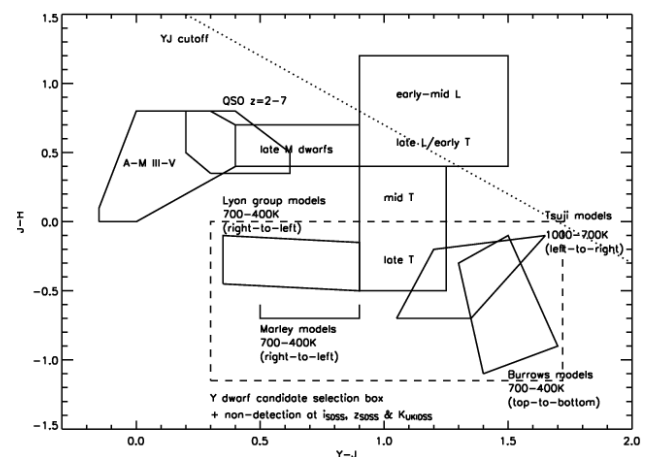


Figure 17. The $J - H$, $Y - J$ two-colour diagram for sources we expect in the WFCAM LAS survey. The location of A-M (III-V) stars, late M, L and T dwarfs and $z=2-7$ QSOs have been determined using colours synthesized from available spectroscopy. Y dwarf colours have been synthesized from the latest theoretical model spectra by the Lyon group (priv. comm.), the Marley group (priv. comm.; see Marley et al. 2002), the Burrows group (Burrows et al., 2003) and Tsuji (priv. comm.). The Lyon $J - H$ colours have been adjusted by -0.3 so that they pass through the known T dwarfs.

manner that T dwarfs are known as methane dwarfs, the next spectral type will be known as ammonia dwarfs.

Figure 17 shows a colour–colour plot with model predictions for Y dwarfs, prepared to aid selecting such objects in the UK Infrared Telescope’s (UKIRT) Wide Field Camera (WFCAM) Large Area Survey (LAS). Although the model groups predict somewhat different colors, we can identify candidate Y dwarfs as red in $Y - J$ and blue in $J - H$ (see also the WFCAM contribution by Leggett in these proceedings). A detailed understanding of Y dwarf properties (and ultimately the brown dwarf mass function) will require spectroscopic analyses to simultaneously determine effective temperature, metallicity and gravity, as we are now attempting for L and T dwarfs.

4.1. DISCUSSION (*All*)

A short contribution on characterization of exoplanetary atmospheres with the VLT Interferometer was presented, see Joergens & Quirrenbach, these proceedings.

REFERENCES

- Ackerman, A. S., Marley, M. S. 2001, ApJ 556, 872
Allard, F., Hauschildt, P. H., Alexander, D. R., Tamanai, A., Schweitzer, A. 2001, ApJ 556, 357
Allard, N. F., Allard, F., Hauschildt, P. H., Kielkopf, J. F., Machin, L. 2003, A&A, 411, L473
Barrado y Navacués, D., Zapatero Osorio, M. R., Béjar, V. J. S. et al. 2001, A&A 337, L9
Burgasser, A. J. 2004, ApJ in press
Burgasser, A. J., Kirkpatrick, J. D., Brown, M. E. et al. 2002, ApJ 564, 421
Burgasser, A. J., Kirkpatrick, J. D., Burrows, A. et al. 2003, ApJ 592, 1186
Burgasser, A. J., Kirkpatrick, J. D., Cutri, R. M. et al. 2000, ApJ 531, L57
Burgasser, A. J., Kirkpatrick, J. D., Liebert, J., Burrows, A. 2003, ApJ 594, 510
Burgasser, A. J., Kirkpatrick, J. D., McGovern, M. R., McLean, I. S., Prato, L., Reid, I. N. 2004, ApJ 604, 827
Burrows, A., Marelly, M. S., Hubbard, W. B. et al. 1997, ApJ 491, 856
Burrows, A., Marley, M. S., Sharp, C. M. 2000, ApJ 531, 438
Burrows A., Sudarsky D., Lunine J. I., 2003, ApJ, 596, 587
Canon A. J., Pickering E. C., 1901, Ann. Astron. Obs. Harvard Coll., 28, 131
Dahn, C. C., Harris, H. C., Vrba, F. J. et al. 2002, AJ 124, 1170
Geballe T. R., Kulkarni S. R., Woodward C. E., Sloan G. C. 1996, ApJ 467, 101
Geballe, T. R., Knapp, G. R., Leggett, S. K. et al. 2002, ApJ 564, 466
Golimowski, D. A., Leggett, S. K., Marley, M. S. et al. 2004, AJ 127, 3516
Gorlova, N., Meyer, M. R., Liebert, J., Rieke, G. H. 2003, ApJ 593, 1074
Jones, H. R. A., Steele I. A. 2001, Ultracool Dwarfs: New Spectral Types L and T, Springer, Heidelberg
Kirkpatrick J. D., 1998, Brown Dwarfs and Extrasolar Planets, ASP 134, 405
Kirkpatrick, J. D., Reid, I. N., Liebert, J. et al. 1999, ApJ 519, 802
Knapp, G. R., Leggett, S. K., Fan, X. et al. 2004, AJ 127, 3553
Leggett, S. K., Golimowski, D. A., Fan, X. et al. 2002, ApJ 564, 452
Lepine, S. Rich, R. M., Shara, M. M. 2003, ApJ 591, L49
Lucas, P. W., Roche, P. F., Allard, F., Hauschildt, P. H. 2001, MNRAS 326, 695
Luhman, K. L., Rieke, G. H. 1999, ApJ 525, 440
Marley, M. 2000, ASP Conf. Ser. 212: From Giant Planets to Cool Stars, 152
Marley, M. S., Seager, S., Saumon, D. et al. 2002 ApJ 568, 335
Martín, E. L., Rebolo, R., Zapatero Osorio, M. R. 1996, ApJ 469, 706
Martín, E. L., Basri, G., Delfosse X., Forveille T., 1997, A&A 327, L29
Martín, E. L., Delfosse, X., Basri, G., Goldman, B., Forveille, T., Zapatero Osorio, M. R. 1999, AJ 118, 2466
Martín, E. L., Zapatero Osorio, M. R., Barrado y Navascués, D., Béjar, V. J. S., Rebolo, R., 2001, 558, L117
Martín, E. L., Zapatero Osorio, M. R. 2003, ApJ 593, L113
Morgan W. W., Keenan P. C., Kellman E., 1943, An Atlas of Stellar Spectra with an Outline of Spectral Classification, Univ. Chicago Press, Chicago
Nakajima T., Oppenheimer, B. R., Kulkarni, S. R., Golimowski, D. A., Matthews, K., Durrance, S. T. 1995, Nature 378, 463
Noll, K. S., Geballe, T. R., Leggett, S. K., Marley M.S. 2000, ApJ 541, 75L
Oppenheimer, B. R., Kulkarni, S. R., Matthews, K., Nakajima, T. 1995, Science 270, 1478
Rebolo, R. Zapatero Osorio, M. R., Madruga, S., Béjar, V. J. S., Arribas, S., Licandro, J. 1998, Science 282, 1309
Roellig, T. L., Van Cleve, J. E., Sloan, G. C. et al. 2004, ApJ Sup. Ser. 154, 418
Saumon, D., Bergeron, P., Lunine, J. I., Hubbard, W. B., Burrows, A. 1994, ApJ 424, 333
Schubert, G., Zhang, K. 2000, ASP Conf. Ser. 212: From Giant Planets to Cool Stars, 210
Slesnick, C. L., Hillenbrand, L. A. H., Carpenter, J. M. 2004, ApJ, in press
Steele, I. A., Jameson, R. F. 1995, MNRAS 272, 630
Tinney, C. G., Burgasser, A. J., Kirkpatrick, J. D. 2003, AJ 126, 975
Tsuji, T. 2002, ApJ 575, 264
Tsuji, T., Nakajima, T. 2003, ApJ 585, L151
Tsuji, T., Nakajima, T., Yanagisawa, K. 2004, ApJ 607, 511
Vrba, F. J., Henden, A. A., Luginbuhl, C. B. et al. 2004, AJ 127, 2948
Zapatero Osorio, M. R., Béjar, V. J. S., Martín, E. L. et al. 2002, ApJ 578, 536